Intercomparison of four methods to estimate coral calcification under various environmental conditions

Miguel Gómez Batista[1], Marc Metian[2], François Oberhänsli[2], Simon Pouil[2], Peter W. Swarzenski[2], Eric Tambutté[3], Jean-Pierre Gattuso[4,5], Carlos M. Alonso Hernández[1], Frédéric Gazeau[4]

[1]Centro de Estudios Ambientales de Cienfuegos, Cuba

[2]International Atomic Energy Agency, Environment Laboratories, 4a Quai Antoine 1er, MC-98000 Monaco, Principality of Monaco

[3]Centre Scientifique de Monaco, Department of Marine Biology, MC-98000 Monaco, Principality of Monaco

[4]Sorbonne Université, CNRS, Laboratoire d'Océanographie de Villefranche, LOV, F-06230 Villefranche-sur-Mer, France

[5]Institute for Sustainable Development and International Relations, Sciences Po, 27 rue Saint Guillaume, F-75007 Paris, France

Correspondence to: Miguel Gómez Batista (mgomezbatista@gmail.com)

Keywords: Calcification; Coral; Alkalinity anomaly; Calcium anomaly; ^{45}Ca incorporation; ^{13}C incorporation

Abstract

Coral reefs are constructed by calcifiers that precipitate calcium carbonate to build their shells or skeletons through the process of calcification. Accurately assessing coral calcification rates is crucial to determine the health of these ecosystems and their response to major environmental changes such as ocean warming and acidification. Several approaches have been used to assess rates of coral calcification, but there is a real need to compare these approaches in order to ascertain that high quality and intercomparable results can be produced. Here, we assessed four methods (total alkalinity anomaly, calcium anomaly, ^{45}Ca incorporation and ^{13}C incorporation) to determine coral calcification of the reef-building coral *Stylophora pistillata*. Given the importance of environmental conditions on this process, the study was performed under two starting pH levels (ambient: 8.05 and low: 7.2) and two light (light and dark) conditions. Under all conditions, calcification rates estimated using the alkalinity and calcium anomaly techniques as well as ^{45}Ca incorporation were highly correlated. Such a strong correlation between the alkalinity anomaly and ^{45}Ca incorporation techniques has not been observed in previous studies and most probably results from improvements described in the present paper. The only method which provided calcification rates significantly different from the other three techniques was ^{13}C incorporation. Calcification rates based on this method were consistently higher than those measured using the other techniques. Although reasons for these discrepancies remain unclear, the use of this technique for assessing calcification rates in corals is not recommended without further investigations.

1. Introduction

Calcification is the fundamental biological process by which organisms precipitate calcium carbonate. Calcifying organisms take up calcium and carbonate or bicarbonate ions to build their biomineral structures (aragonite, calcite and/or vaterite) which have physiological, ecological and biogeochemical functions. Moreover, calcium carbonate plays a major role in the services provided by ecosystems to human societies.

The ocean has absorbed large amounts of anthropogenic CO_2 since the start of the industrial revolution and is currently sequestering about 22% of CO_2 emissions (average 2008-2017; Le Quéré et al., 2018). This massive input of CO_2 in the ocean impacts seawater chemistry with a decrease in seawater pH, carbonate ion concentrations [CO_3^{2-}] and an increase in CO_2 and bicarbonate concentrations [HCO_3^-]. These fundamental changes to the carbonate system are referred to as "ocean acidification" (OA; Gattuso and Hansson, 2011). Models project that the average surface water pH will drop by 0.06 to 0.32 pH units by the end of the century (IPCC, 2014).

The effect of OA is currently the subject of intense research with particular attention to organisms producing $CaCO_3$. For instance, coral communities have already proven to be particularly vulnerable to rapidly changing global environmental conditions (e.g. Albright et al., 2018). In order to help project the future of coral reefs, accurate estimates of calcification rates during realistic perturbation experiments are necessary in order to produce high quality and intercomparable results (Cohen et al., 2017; Gazeau et al., 2015; Langdon et al., 2010; Riebesell et al., 2010; Schoepf et al., 2017).

Several methods are available to quantify rates of coral calcification. Calcification can be measured as the increase of $CaCO_3$ mass (e.g. the buoyant weight technique; Jokiel et al.,

66 1978) or following the incorporation of radio-labelled carbon or calcium in the skeleton
67 (Goreau, 1959), but also through the quantification of changes in a seawater constituent that is
68 stoichiometrically related to the amount of $CaCO_3$ precipitated. For instance, the alkalinity
69 anomaly technique (Smith and Key, 1975) has been widely used to estimate net calcification
70 of organisms and communities, especially of corals and coral reef environments (e.g. Smith
71 and Kinsey, 1978; Gazeau et al., 2015; Albright et al., 2016; Cyronak et al., 2018). Total
72 alkalinity (A_T) is directly influenced by bicarbonate and carbonate ion concentrations together
73 with a multitude of other minor compounds (Wolf-Gladrow et al., 2007). Calcification
74 consumes carbonate or bicarbonate, following the reversible reaction:

75 $$Ca^{2+} + 2HCO_3^- \leftrightarrow CaCO_3 + CO_2 + H_2O \quad (1)$$

76 Calcification consumes two moles of HCO_3^-, hence decreasing A_T by two moles per
77 mole of $CaCO_3$ produced (eq. 1). It is possible to derive the rate of net calcification (gross
78 calcification - dissolution) by measuring A_T before and after incubating an organism or a
79 community. This method assumes, however, that calcification is the only biological process
80 influencing A_T (Smith and Key, 1975). Nitrogen assimilation through photosynthetic
81 activities, nitrification as well as aerobic and anaerobic remineralization of organic matter are
82 known to impact A_T through the consumption or release of nutrients (ammonium, nitrate and
83 phosphate) and protons (Wolf-Gladrow et al., 2007). While for some group of species (e.g.
84 bivalves, sea urchins), corrections appear necessary to take into account the effect of nutrient
85 release on A_T, changes in nutrient concentrations during incubations of isolated corals are too
86 low (i.e. several orders of magnitude lower than changes in A_T) to introduce a significant bias
87 in the calculations (Gazeau et al., 2015).

88 In contrast to A_T, the concentration of calcium (Ca^{2+}) in seawater is only biologically
89 influenced by net calcification and a 1:1 relationship can be used to derive net calcification

rates (eq. 1). The depletion of A_T and Ca^{2+} needs to be corrected for gains of A_T and Ca^{2+} resulting from evaporation. These corrections can be applied through the incubation of seawater in the absence of coral (Schoepf et al., 2017). Both the alkalinity anomaly and calcium anomaly methods are non-destructive and typically show a good agreement (Chisholm and Gattuso, 1991; Murillo et al., 2014; Gazeau et al., 2015).

The ^{45}Ca incorporation technique has been used since the 1950's (Goreau and Bowen, 1955; Goreau, 1959). While earlier techniques showed low reproducibility, methodological improvements led to a significant reduction of the deviations between replicates (see Tambutté et al., 1995, for more details). The strength of this method is that it is extremely sensitive for measuring short-term variations in gross calcification rates. However, in contrast to the A_T and Ca^{2+} anomaly techniques, it is a sample-destructive method.

Previous studies designed to compare calcification rate estimates using the ^{45}Ca incorporation and A_T anomaly methods revealed subtle discrepancies. For example, Smith and Roth in Smith and Kinsey (1978) reported an overestimation of rates based on the ^{45}Ca method. In contrast, Tambutté et al. (1995) and Cohen et al. (2017) reported a decrease in A_T without concomitant incorporation of ^{45}Ca; therefore, suggesting an overestimation of calcification derived from A_T measurements. However, during these studies, in order to avoid radioactive contamination of laboratory equipment, estimates of calcification were not performed during the same incubations, but rather during incubations performed over two consecutive days.

In contrast to the ^{45}Ca incorporation method, to the best of our knowledge, no studies have used carbon-based incorporation techniques to estimate coral calcification rates in the framework of ocean acidification. Past studies that compared carbon and calcium incorporation rates in coral skeletons based on a double labelling technique with $H^{14}CO_3$ and

114 ^{45}Ca showed that only a minor proportion of the labelled seawater carbon is incorporated in
115 the skeleton (e.g. Marshall and Wright, 1998) and that the major source of dissolved inorganic
116 carbon for calcification is metabolic CO_2 (70–75% of the total $CaCO_3$ deposition; Furla et al.,
117 2000). Consequently, under both light and dark conditions, the rate of ^{45}Ca deposition appears
118 greater than the rate of ^{14}C incorporation (Furla et al., 2000). To the best of our knowledge,
119 only one study estimated calcification rates of a benthic calcifier (coralline algae) using a
120 stable carbon isotopic technique through addition of ^{13}C-labelled bicarbonate (McCoy et al.,
121 2016). The present study aimed at comparing calcification rates measured using the alkalinity
122 and calcium anomaly methods, as well as the ^{45}Ca and ^{13}C incorporation techniques, under
123 different pH and light conditions.

2. Material and Methods

Colonies of the reef-building coral *Stylophora pistillata* were incubated in the laboratory, both in the light and dark, under ambient and lowered pH conditions. At ambient pH (experiment conducted in July-August 2017), two sets of incubations were performed using either ^{45}Ca or ^{13}C additions and calcification rates based on these techniques were compared to those derived, during the same incubations, by the alkalinity and calcium anomaly techniques. At lowered pH (experiment conducted in August 2018), no incubations with ^{13}C addition were conducted and only the three other techniques were compared.

2.1. Biological material and experimental set-up

Specimens used in this experiment originated from colonies of the coral *Stylophora pistillata* (Esper 1797) initially sampled in the Gulf of Aqaba (Red Sea, Jordan) and transferred to the Scientific Centre of Monaco where they were cultivated under controlled conditions for several years. In June 2017, 40 terminal portions branches of *S. pistillata*, free of boring organisms, were cut from four different parent colonies (10 branches per parent colony) and suspended by nylon lines to allow tissues to fully cover the exposed skeleton for at least five weeks (Tambutté et al., 1995; Houlbrèque et al., 2015). The nubbins were fed with rotifers (once a day) and Artemia nauplii (twice a week; ca. 1 nauplius mL^{-1}) and kept in 70 L aquaria (water renewal: 2 L min^{-1}) under an irradiance of 200 µmol photons m^{-2} s^{-1} (12:12 light:dark photoperiod, light banks: HQI 250W Nepturion - BLV (Germany) / 200 µmol photons m^{-2} s^{-1}), a seawater temperature of 25 ± 0.5 °C and a salinity of 38 ± 0.5. Water motion was provided by a submersible pump (Minijet MN 606; RENA©). Before the start of the experiment, specimens were transferred to the International Atomic Energy Agency

146 (IAEA). For the second set of experiments in 2018, nubbins were prepared in June 2018 and
147 cultured, under the conditions described above, at IAEA except that colonies were fed twice a
148 week with newly hatched brine shrimp nauplii (ca. 1 nauplius mL^{-1}). Biometrics parameters
149 (size, weight) of the biological material are shown in Table 1.

150 Different types of incubations were conducted. In July-August 2017, one set of
151 incubations was performed under ambient pH conditions with the addition of radioactive
152 calcium dichloride ($^{45}CaCl_2$). During the same period, another set of incubations was
153 performed, under ambient pH conditions, with addition of labelled ^{13}C-sodium bicarbonate
154 (^{13}C-$NaHCO_3$ 99%). Finally, in August 2018, one set of incubations was performed under
155 lowered pH conditions (see thereafter for more details) with the addition of $^{45}CaCl_2$. For all
156 sets of incubations, organisms were incubated for 5 to 11 hours (Table 1), both in the light
157 and dark, in 500 mL polyethylene beakers equipped with a magnetic stirrer (Fig. 1). Six and
158 five replicates were used, respectively, at ambient and low pH. Furthermore, for all sets of
159 incubations, one beaker was incubated, under the same conditions as the other beakers,
160 without coral and served as a control.

161 For each set of incubations, 2.4 L of seawater, pumped continuous from offshore of
162 the IAEA Monaco premises at 60 m depth, were filtered onto 0.2 µm (GF/F, 47 mm). For
163 incubations performed at lowered pH condition, pure CO_2 was bubbled in the 2.4 L initial
164 seawater batch using an automated pH-stat system (IKS Aquastar©) until the target pH was
165 reached. The pH electrode from the pH-stat system was inter-calibrated using a glass
166 combination electrode (Metrohm, Ecotrode Plus) calibrated on the total scale using a TRIS
167 buffer solution with a salinity of 35 (provided by A. Dickson, Scripps Institution of
168 Oceanography, San Diego). Initial pH_T (total scale) levels were set to ~7.2. It must be stressed
169 that pH levels were not regulated during the incubations. For ^{45}Ca-incubations, this initial

batch was spiked with $^{45}CaCl_2$ to reach a nominal activity of ~15 Bq mL^{-1}. As we anticipated lower calcification rates during the set of experiments conducted at low pH, initial nominal activity was set to ~30 Bq mL^{-1}. Before distributing seawater to the experimental beakers, a one-milliliter aliquot of seawater was removed for the precise determination of the initial activity. Samples were stored, in the dark, in high-performance glass vials for 24 h before counting. For ^{13}C-incubations, to determine seawater background isotopic level ($\delta^{13}C$) of the dissolved inorganic carbon pool ($\delta^{13}C$-C_T), three 27 mL samples were collected and gently transferred to glass vials avoiding bubbles. Then, ~8.95 mg of ^{13}C-$NaHCO_3$ were added to the batch of filtered ambient seawater to increase $\delta^{13}C$-C_T to ca. 1,500‰. For the determination of $\delta^{13}C$-C_T after enrichment, two 27 mL samples were handled as described above. The vials were then sealed after being poisoned with 10 µL of saturated mercuric chloride ($HgCl_2$) and stored upside-down at room temperature in the dark for subsequent analysis.

For all sets of incubations, samples for the measurements of pH_T, A_T (200 mL), and Ca^{2+} concentrations (50 mL) were taken before distributing seawater to the experimental beakers. While pH_T was measured immediately after sampling, samples for A_T measurements were poisoned with 40 µL of 50% saturated $HgCl_2$ and stored in the dark at 4 °C pending analysis less than two weeks later. Samples for [Ca^{2+}] measurements were not poisoned and stored in the dark at 4 °C pending analysis less than two weeks after sampling.

Gravimetrically determined amounts of filtered seawater (ca. 300 g) were transferred to the incubation containers which were placed in a temperature-controlled (IKS Aquastar©) water bath maintained at 25 ± 0.5 °C. Coral nubbins were suspended with a nylon line in the experimental beakers 5 cm below the water level covered with transparent film to limit evaporation (Fig. 1). During the low pH incubations conducted in 2018, to avoid physiological stress, coral nubbins were acclimated by gradually lowering pH to the target

194 levels during 24 h. This acclimation was performed in an open-flow 20 L aquarium (one full
195 water renewal per hour) using a pH-stat system as previously described and with a pH
196 decrease of ca. 0.03 units h^{-1}.

197 Incubations in the light were performed at an irradiance of 200 µmol photons m^{-2} s^{-1}
198 during daytime whereas dark incubations were conducted at night. Incubation times were not
199 fixed based on scientific considerations and differed between the different incubations due to
200 practical constrains (i.e. access to the lab etc…). Before the beginning of the incubations, all
201 beakers (containing corals) were precisely weighed at ± 0.01 g (Sartorius BP 310S).

202 At the conclusion of the incubations, all beakers were precisely weighed to evaluate
203 evaporation and seawater samples were analyzed for pH_T, A_T and $[Ca^{2+}]$ as well as for ^{45}Ca
204 activity or $\delta^{13}C$-C_T depending on the type of incubations. pH_T was measured immediately and
205 samples for A_T and $[Ca^{2+}]$ determinations were filtered onto 0.2 µm (GF/F, Ø 47 mm),
206 poisoned with saturated $HgCl_2$ (only for A_T) and stored in the dark at 4 °C pending analysis
207 (within two weeks). The corals were then removed from the beakers for the analysis of
208 incorporated ^{45}Ca or ^{13}C. Three additional corals which were not incubated were processed
209 for carbon isotopic composition of the previously accreted calcium carbonate (see section
210 "2.3. Computations and statistics").

211 2.2. Analytical techniques

212 Immediately after sampling, pH_T was measured on a Metrohm 826 mobile pH-logger
213 and a glass electrode (Metrohm, Ecotrode Plus) calibrated on the total scale using a TRIS
214 buffer of salinity 35 (provided by A. Dickson, Scripps University, USA). A_T was determined
215 in triplicate 50 mL subsamples by potentiometric titration on a titrator Titrando 888
216 (Metrohm) coupled to a glass electrode (Metrohm, Ecotrode Plus) and a thermometer

(pt1000). The pH electrode was calibrated before every set of measurements on the total scale using a TRIS buffer of salinity 35 (provided by A. Dickson, Scripps University, USA). Measurements were carried out at a constant temperature of 25 °C and A_T was calculated as described in Dickson et al. (2007). Certified reference material (CRM; batches 143 and 156) provided by A. Dickson (Scripps University, USA) were used to check precision (standard deviation within measurements of the same batch) and accuracy (deviation from the certified nominal value). Over the six series of A_T measurements performed during the experiment, mean accuracy and precision (± SD) were respectively 7.2 ± 1.2 and 1.2 ± 0.2 μmol kg^{-1}. $[Ca^{2+}]$ was determined in triplicate using the ethylene glycol tetra acetic acid (EGTA) potentiometric titration (Lebel and Poisson, 1976). About 10 g of sampled seawater and 10 g of $HgCl_2$ solution (ca. 1 mmol L^{-1}) were accurately weighed out. Then, about 10 g of a concentrated EGTA solution (ca. 10 mmol L^{-1}, also by weighing) was added to completely complex Hg^{2+} and to complex nearly 95% of Ca^{2+}. After adding 10 mL of borate buffer (pH_{NBS} ~ 10) to increase the pH of the solution, the remaining Ca^{2+} was titrated by a diluted solution of EGTA (ca. 2 mmol L^{-1}) using a tritrator (Titrando 888, Metrohm) coupled to an amalgamated silver combined electrode (Metrohm Ag Titrode). Following Cao and Dai (2011), the volume of EGTA necessary to titrate the remaining ca. 5% of Ca^{2+} were obtained by manually fitting a polynomial function to the first derivative of the titration curve using the function "loess" of the R software[1]. The EGTA solution was calibrated prior to each measurement series using International Association for the Physical Sciences of the Oceans (IAPSO) standard seawater (salinity = 38.005). Mean $[Ca^{2+}]$ precision obtained using this technique was 2.9 μmol kg^{-1} (n = 40), corresponding to a coefficient of variation (CV) of 0.026%.

[1]The R Development Core Team, R.: A language and environment for statistical computing, 2018.

To determine the specific activity in radio-labelled seawater, the 1 mL aliquots were transferred to 20 mL glass scintillation vials and mixed in proportion 1:10 (v:v) with scintillation liquid Ultima Gold ^{TM} XR. According to a method adapted from Tambutté et al. (1995), at the end of incubation sampled nubbins were immersed for 30 min in beakers containing 300 mL of unlabelled seawater to achieve isotopic dilution of the ^{45}Ca contained in the gastrovascular cavity. Constant water motion was provided in the efflux medium by magnetic stirring bars. Tissues were then dissolved completely in 1 mol L^{-1} NaOH at 90 °C for 20 min. The skeleton was rinsed twice in 1 mL NaOH and twice in 5 mL in MilliQ water. It was then dried for 72 h at 60 °C, precisely weighed at ± 0.01 g using a Sartorius BP 310S (referred thereafter to as skeleton dry weight), and dissolved in 12 N HCl. Three 200 µL aliquots from each skeleton dissolution were transferred to 20 mL glass scintillation vials and mixed with 10 mL scintillation liquid Ultima Gold ^{TM} XR. Radioactive samples were thoroughly mixed to homogenize the solution and kept in the dark for 24 h before counting. The radioactivity of ^{45}Ca was counted using a Tri-Carb 2900 Liquid Scintillation Counter. Counting time was adapted to obtain a propagated counting error of less than 5% (maximal counting duration was 90 min). Radioactivity was determined by comparison with standards of known activities and measurements were corrected for counting efficiency and physical radioactive decay.

The analyses of seawater $\delta^{13}C$-C_T as well as of the ^{13}C signature of coral calcified tissues were performed at Leuven University. For $\delta^{13}C$-C_T analyses, a helium headspace (5 mL) was created in the vials and samples were acidified with 2 mL of phosphoric acid (H_3PO_4, 99%). Samples were left to equilibrate overnight to transfer all C_T to gaseous CO_2. Samples were injected in the carrier gas stream of an EA-IRMS (Thermo EA1110 and Delta V Advantage), and data were calibrated with NBS-19 and LSVEC standards (Gillikin and

Bouillon, 2007). Corals were treated following the same protocol as for ^{45}Ca incorporation measurements and powdered. Triplicate subsamples of carbonate powder (~100 μg) were placed into gas-tight vials, flushed with helium, and converted into CO_2 with H_3PO_4. After 24 h, subsamples of the released CO_2 were injected into the EA-IRMS system as described above. Data were calibrated with NBS-19 and LSVEC. Carbon isotope data are expressed in the delta notation (δ) relative to Vienna Pee Dee Belemnite (VPDB) standard and were calculated as:

$$R_{sample} = \frac{\delta^{13}C_{sample}}{1000 + 1} \cdot R_{VPDB} \quad (2)$$

2.3. Computations and statistics

The carbonate chemistry was assessed using pH_T and A_T and the R package seacarb[2]. Propagation of errors on computed parameters was performed using the new function "error" of the package seacarb (Orr et al., 2018) on the R software, considering errors associated to the estimation of A_T as well as errors on dissociation constants.

Estimates of coral calcification rates based on changes in A_T and $[Ca^{2+}]$ during incubations were computed following equations (3) and (4), respectively. As shown in these equations, initial levels of A_T and $[Ca^{2+}]$ are not necessary to compute calcification rates and only final values in the incubations with corals and without corals (controls) were used:

$$G_{AT} = -\frac{(A_{T2} - A_{T1}) - (A_{T2c} - A_{T1})}{2t} \cdot \frac{W_w}{W_c} = -\frac{(A_{T2} - A_{T2c})}{2t} \cdot \frac{W_w}{W_c} \quad (3)$$

$$G_{Ca} = -\frac{(Ca_2 - Ca_1) - (Ca_{2c} - Ca_1)}{t} \cdot \frac{W_w}{W_c} = -\frac{(Ca_2 - Ca_{2c})}{t} \cdot \frac{W_w}{W_c} \quad (4)$$

[2]seacarb: seawater carbonate chemistry with R. Gattuso, J.-P., J. M. Epitalon, H. Lavigne, J. C. Orr, B. Gentili, M. Hagens, A. Hofmann, A. Proye, K. Soetaert and J. Rae, 2018. https://cran.r-project.org/package=seacarb

where A_{T1} and Ca_1 are A_T and Ca^{2+} concentrations at the start of the incubations (in µmol kg^{-1}; not used in the computations), A_{T2}/A_{T2c} and Ca_2/Ca_{2c} are A_T and Ca^{2+} concentrations at the end of the incubations, respectively with and without corals, t is the incubation duration in h, W_w and W_c are respectively the mass of seawater (average between initial and final weights) and the coral skeleton dry weight (g; DW). G_{AT} and G_{Ca} are therefore expressed in µmol $CaCO_3$ g DW^{-1} h^{-1}. Error propagation was used to estimate errors:

$$SE_{G_{AT}} = \frac{\sqrt{SE_{AT_2}^2 + SE_{AT_{2c}}^2}}{2t} \cdot \frac{W_w}{W_c} \quad (5)$$

$$SE_{G_{Ca}} = \frac{\sqrt{SE_{Ca_2}^2 + SE_{Ca_{2c}}^2}}{t} \cdot \frac{W_w}{W_c} \quad (6)$$

where $SE_{AT_2}/SE_{AT_{2c}}$ and $SE_{Ca_{2c}}/SE_{Ca_{2c}}$ correspond to standard errors associated with the measurement of three analytical replicates per sample for A_T and Ca^{2+} at the end of the incubations, respectively with and without corals, t is the incubation duration in h, W_w and W_c are respectively the mass of seawater (average between initial and final weights) and the coral skeleton dry weight (g DW).

Coral calcification rates based on ^{45}Ca incorporation were estimated using measured seawater activity and activity recorded in the skeleton digest. Rates were then normalized per g skeleton dry weight using the formula:

$$G_{45Ca} = \frac{Activity_{sample} \cdot \frac{Ca}{Activity_{seawater}}}{W_c \cdot t} \quad (7)$$

where $Activity_{sample}$ is the average of counts per minute (CPM) of three 200 µL aliquots from the dissolved skeleton sample, $Activity_{seawater}$ is the total CPM in the 1 mL seawater samples, Ca is the $[Ca^{2+}]$ measured in the corresponding samples (average between initial and final values, µmol kg^{-1}) and further converted to µmol L^{-1} considering a

304 temperature of 25 °C and a salinity of 38, W_c is the skeleton dry weight (in g) and t the
305 incubation duration (h). G_{45Ca} is therefore expressed in μmol $CaCO_3$ g DW^{-1} h^{-1}. The standard
306 errors for these calcification rate estimates were propagated based on standard errors
307 associated with the measurements of triplicate samples for both $Activity_{sample}$ and $[Ca^{2+}]$.

308 The precipitation of calcium carbonate minerals (G) during the incubation interval was
309 also estimated using measured $\delta^{13}C$ values and isotope mass balance calculations [eq. (8) and
310 (9) below]. The CO_2 released during phosphoric acid digestion is derived from two sources:
311 new coral $CaCO_3$ and previously accreted skeletal carbonate mineral. The new carbon
312 acquired in each measured nubbins ($\delta^{13}C_N$) was assumed to have the same carbon isotope
313 composition as the labelled seawater C_T (average between initial and final level, $\delta^{13}C$-C_T ~
314 1,400-1,700‰). The previously accreted skeletal material was assumed to have a $\delta^{13}C$ value
315 equal to the measured value for the background sample ($\delta^{13}C_P$). The $\delta^{13}C$ value ($\delta^{13}C_M$),
316 representing the mixture of new calcified material and previously accreted carbonate mineral,
317 is then calculated the following mixing equation:

318 $$\delta^{13}C_M = f_G \cdot \delta^{13}C_N + (1 - f_G) \cdot \delta^{13}C_P \quad (8)$$

319 where f_G is the fraction of the calcium carbonate mineral precipitated during the experiment,
320 and $\delta^{13}C_N$ and $\delta^{13}C_P$ are the carbon isotope compositions of the newly precipitated and
321 previously accreted calcium carbonate, respectively. Equation (8) was solved for f_G to
322 determine the calcium carbonate precipitated during the incubation using:

323 $$G_{13_C} = \frac{f_G}{t \cdot M_{CaCO_3}} \cdot 1e^6 \quad (9)$$

where M_{CaCO3} is the molar mass of calcium carbonate (g mol^{-1}) and t is the incubation duration in h. G_{13C} are therefore expressed in µmol $CaCO_3$ g DW^{-1} h^{-1}. The standard errors for these calcification rate estimates were calculated based on standard errors associated with the triplicate measurements of $\delta^{13}C_P$ and $\delta^{13}C_N$.

Model-II linear regressions (Sokal and Rohlf, 1995) were used to compare net calcification rates obtained with the different methods. All regressions were performed using function "lmodel2" of the package lmodel2[3] on the R software.

[3]lmodel2: Model II Regression, Legendre P. and J. Oksanen, 2018. https://cran.r-project.org/package=lmodel2

3. Results

Environmental conditions at the start of the different incubations are shown in Table 2. All values in Table 2 as well as in the text below correspond to the average between replicates (or incubations) ± standard deviation (SD). All incubations performed under ambient pH_T (~8.05) were conducted under carbonate chemistry favorable to calcification with saturation states with respect to aragonite (Ω_a) well above 1 (average of 4.0 ± 0.1 over the four incubations). In contrast, during experiments at low pH_T (initial pH_T ~ 7.2), seawater was corrosive with respect to aragonite (Ω_a ~ 0.75). However, as pH was not regulated during the incubations (see previous section), it increased, at lowered pH, to an average of 7.75 ± 0.03 (n = 5) in dark conditions and to an average of 7.84 ± 0.03 in light conditions (n = 5). Evolution of pH in control beakers (final pH_T of 7.78 and 7.48; n = 1 for both in the light and in the dark, respectively) showed that the observed increase in beakers with corals was due to the additive effects of biological control (photosynthesis minus respiration and calcification) and exchanges at the interface in the light, and mostly due to CO_2 exchange with air during the much longer incubations performed in the dark. Assuming linear variations with time, the average conditions of the carbonate chemistry in the lowered pH experiments were slightly favorable to aragonite production (Ω_a = 1.4 ± 0.2 in the dark, n = 5 and 1.6 ± 0.05 in the light, n = 5). Under ambient pH conditions (both for ^{45}Ca and ^{13}C incubations), pH did not change during incubations in the light (average final pH_T of 8.05 ± 0.03, n = 12, data not shown) while it decreased in the dark, due to respiration and calcification, to reach an average pH_T level of 7.62 ± 0.07, n = 12, data not shown). In control beakers under ambient pH, pH_T slightly increased in the light (8.09, n = 2) and did not change in the dark (8.05, n = 2).

353 ^{45}Ca activities in seawater did not change during the incubations, reaching a final
354 activity of 16.1 ± 1.2 (n = 12) and 28.5 ± 0.6 (n = 10) Bq mL^{-1} under ambient and lowered pH
355 conditions, respectively (including both dark and light incubations, data not shown).
356 Furthermore, for all incubations, these values were similar to those measured in beakers
357 without corals (control, data not shown). Under ambient pH levels (no incubation at lowered
358 pH), seawater was enriched in ^{13}C ($\delta^{13}C$-C_T) from a background level of 0.26 ± 0.05‰ (n = 3)
359 to 1,740 ± 4.7‰ (n = 2) and 1,634 ± 11‰ (n = 2) in the light and dark, respectively. During
360 light condition incubations, $\delta^{13}C$-C_T levels decreased to an average of 1,636 ± 10‰ (n = 6,
361 data not shown) while they decreased to an average of 1,466 ± 24‰ in dark conditions (n = 6,
362 data not shown). Incubations in control beakers (without corals) showed that the majority of
363 $\delta^{13}C$-C_T loss for both types of incubations (light and dark) was due to ^{13}C incorporation by
364 corals with a minor effect of gas exchanges at the interface (data not shown).
365 Both A_T and $[Ca^{2+}]$ declined in all incubations as a consequence of coral calcification
366 (Table 3). Changes in A_T during incubations in control beakers (data not shown) were
367 comprised between 0.1 and 1.1% of the initial level. Similar results were observed for $[Ca^{2+}]$
368 with a relative change comprised between 0.05 and 1.15% of the initial value. These minimal
369 changes were corroborated with no measurable changes in seawater weight between the start
370 and the end of all incubations (data not shown), showing that evaporation, if any, was
371 minimal using our experimental set-up over the considered incubation times. At ambient pH
372 levels, decreases in A_T and $[Ca^{2+}]$ (average of -380 ± 97 and -194 ± 51 μmol kg^{-1} for both
373 parameters, respectively, n = 24 including both ^{45}Ca and ^{13}C incubations) were roughly
374 similar under light and dark conditions although coral specimen used for dark incubations
375 were ca. 166% heavier (skeleton dry weight, see Table 1). Incubations performed under
376 lowered pH levels showed much lower A_T and $[Ca^{2+}]$ net consumption rates than under

ambient pH levels. Under these pH conditions, an extremely high A_T consumption rate was observed in one beaker (dark incubation, see Table 3) while no changes in [Ca^{2+}] was observed in a total of three beakers (see Table 3). These estimates (n = 4) have been considered as outliers, marked with an asterisk in Table 3 and not included in the following analyses.

^{45}Ca activities in coral skeleton reached maximum levels under ambient pH and light conditions (average of 87.5 ± 9.1 Bq, n = 6). Although seawater was more enriched in ^{45}Ca at the lower pH levels (see above), ^{45}Ca activity in corals incubated under these conditions were much lower with lowest values measured in the dark (average of 19.6 ± 9.1 Bq, n = 5). $\delta^{13}C$ levels measured in coral skeletons (-3.69 to 8.92‰) showed significant enrichment as compared to background levels (-3.97 ± 0.35‰, n = 9).

Calcification rates using the different techniques were higher in the light than in the dark and much lower rates were estimated at lowered pH (Table A1, Figs. 2, 3 and 4). The rates measured by alkalinity anomaly (G_{AT}) and calcium anomaly (G_{Ca}) techniques were highly correlated (Fig. 2; $R^2 = 0.98$, $p < 0.01$, n = 34). No significant difference was observed between rates measured by the two methods (see Table 4 for the 95% confidence intervals of the slope and intercept). The ^{45}Ca method provided also very similar rates than the two previous approaches (Fig. 3; G_{Ca} vs. G_{45Ca} not shown) although the slope and the intercept of the geometric regression between G_{AT} and G_{45Ca} were significantly different from 1 and 0, respectively. Finally, the only approach that did not provide similar rates to the others was the ^{13}C incorporation technique. Calcification rates based on this method were systematically higher than those measured using the other three techniques (see Table 4), and rates were not always significantly related (e.g. $R^2 = 0.33$, $p > 0.05$, n = 12 for G_{AT} vs. G_{13C}, see Fig. 4; other relationships not shown).

4. Discussion

Under all experimental conditions (ambient pH vs. low pH, light vs. dark), significant consumption rates of A_T and Ca^{2+} as well as significant incorporation rates of ^{45}Ca and ^{13}C were observed in the zooxanthellate coral *Stylophora pistillata*. For all methods, calcification rates were lower in dark than in light conditions. Such trends are expected as it has long been established that calcification rates increase in zooxanthellate corals during periods in which photosynthesis is occurring (Yonge, 1931), a process known as light-enhanced calcification (e.g. Gattuso et al., 1999). Even under lowered pH conditions, at pH levels far below those predicted to occur in the next decades (starting pH_T of ca. 7.2, average pH_T during incubations of ca. 7.5), all corals appeared to produce calcifying structures under both light and dark conditions. The organisms selected for this experiment were fully coated with tissues with no exposed calcareous structures which can explain the absence of observable net dissolution such as reported by Cohen et al. (2017) in a similar study. Since our experimental protocol was not designed to address the potential impact of decreasing pH levels on calcification rates of this species (no control of carbonate chemistry during incubations, no acclimation of the organisms etc.), we will not discuss further the observed decrease of calcification rates identified by the three techniques used at these pH levels.

Under all experimental conditions, rates of calcification calculated using the alkalinity and the calcium anomaly techniques were highly correlated with a slope of 1 and no significant intercept. These results are consistent with previously published data on colonies of *Pocillopora damicornis* (Chisholm and Gattuso, 1991), *Cladocora caespitosa* (Gazeau et al., 2015) and several other coral species (Murillo et al., 2014). Although the precision obtained on Ca^{2+} measurements is among the highest reported to date (Gazeau et al., 2015),

424 the alkalinity anomaly technique appears as the most appropriate to estimate calcification
425 rates of isolated corals (better precision, stronger signals). As observed by Murillo et al.
426 (2014), this is not true when an entire community including sediment is investigated. The
427 occurrence of several processes in the sediment that can impact A_T prevents the use of this
428 technique. It is therefore recommended to use the calcium anomaly technique when working
429 in natural settings, assuming that Ca^{2+} concentrations are measured with an analytical
430 technique as precise as the one used in our study (CV < 0.05%). Similarly, although
431 corrections are possible when applying the alkalinity anomaly technique on organisms that
432 significantly release nutrients (echinoderms, bivalves etc.), the use of the calcium anomaly
433 technique is highly recommended instead (Gazeau et al., 2015).

434 Calcification rate estimates based on changes of A_T or Ca^{2+} were highly correlated
435 with estimates based on ^{45}Ca incorporation in corals. These results are not consistent to those
436 reported by Smith and Roth (in Smith and Kinsey, 1978), Tambutté et al. (1995) and Cohen et
437 al. (2017). These studies revealed discrepancies between the alkalinity anomaly and the ^{45}Ca
438 incorporation techniques. Smith and Roth found that rates measured with the ^{45}Ca method
439 were higher than those measured using the alkalinity anomaly technique (significant ^{45}Ca
440 incorporation at $\Delta A_T = 0$). Results from both Tambutté et al. (1995) and Cohen et al. (2017)
441 suggested the opposite with a decrease in A_T consumption without any concomitant ^{45}Ca
442 incorporation. A number of reasons may explain these discrepancies. First, the present study
443 is the first one comparing these techniques in the same incubations, in contrast to the other
444 ones in which incubations for A_T anomaly and ^{45}Ca incorporation were performed over two
445 consecutive days (due to radioactive contamination issues). Second, calcification expressed as
446 absolute changes in A_T during incubations, measured during our experiment, were at least one
447 order of magnitude higher than measured during these studies (44,200 to 745,600 nmol vs.

448 less than 4,000 nmol in previous experiments). Cohen et al. (2017) have shown that such
449 discrepancies were much higher at very low rates and that the ratio between rates estimated
450 based on ^{45}Ca incorporation and A_T consumption were getting closer to 1 with increasing
451 calcification rates. Nevertheless, even at the highest levels of calcification computed during
452 these studies, ^{45}Ca-based rates were still significantly different from ΔA_T-based rates, which is
453 in contrast with our results.

454 As already mentioned, although calcification rates of the present study were lower at
455 lowered pH levels, there was still a close to perfect agreement between the different
456 techniques. While the ^{45}Ca labelling technique is thought to provide rates of gross
457 calcification, there is no doubt that both the A_T and Ca^{2+} anomaly techniques allow the
458 estimation of net calcification rates (gross calcification – dissolution). A full agreement of
459 rates computed from these methods further suggest that no dissolution of previously
460 precipitated $CaCO_3$ structures occurred during our study, even under lowered pH conditions.
461 The corals used in our experiment were fully covered with tissues which is likely the reason
462 why no dissolution was measured.

463 Furthermore, we must note that the protocol for ^{45}Ca incorporation considered in our
464 study differed from the one used in the above-mentioned past studies. A much smaller activity
465 was used (0.025 kBq mL^{-1}) compared to Tambutté et al. (1995; 40 kBq mL^{-1}) and Cohen et al.
466 (2017; 9 kBq mL^{-1}). Moreover, in contrast to Cohen et al. (2017), rates were not corrected for
467 ^{45}Ca incorporation on the skeleton of dead corals. This choice was motivated by the absence
468 of detectable radioactivity on bare skeletons exposed for 7 h and treated with the same
469 protocol than one used in our study (Lanctôt, pers. comm.).

470 To the best of our knowledge, this is the first study comparing calcification rates
471 measured using the ^{13}C labelling technique to the more widely used alkalinity and calcium

anomaly techniques. It shows that ^{13}C-derived rates were systematically higher and much more variable (with large uncertainties) than the ones estimated using the two other techniques. As already mentioned, several studies have shown that most of the carbon precipitated in the skeleton comes from coral and its symbiotic zooxanthellae (e.g. Erez, 1978; Furla et al., 2000), leading to an underestimation of calcification rates based on labelled, radioactive carbon incorporation. As there is no reason for ^{13}C to behave differently, our results appear inconsistent with a metabolic source of carbon. As the nubbins were treated following the same protocol as for ^{45}Ca incorporation measurements, it is unclear why much stronger ^{13}C incorporation was obtained and why variability was so high. Before better insights on such discrepancies can be developed, we recommend to avoid this technique to estimate coral calcification rates.

Our study was designed to compare different techniques to estimate calcification rates and not to define the best experimental approach to study the effects of ocean acidification on coral species using these different approaches. As such, the chosen experimental protocol (e.g. incubation times) was not optimal and led, in some cases, to significant changes in the carbonate chemistry during incubations. However, our results provide some insights that we further discuss in the following section. Measuring and comparing calcification rates of organisms under varying pH conditions requires the careful choice of a volume and a time interval such that the precision of the calcification rate measurement is large enough to observe significant signals and that the change in carbonate chemistry parameters between the beginning and end of the incubation is small compared to the range of these parameters in the different treatments (Langdon et al., 2010). Table 5 illustrates the incubation time necessary to obtain measurable changes for each method (t_{min}) considering the ratio between incubation volume and coral size chosen for our study. As the ^{13}C incorporation method did not provide

496 reliable rates, this technique was not considered in this analysis. The threshold for significant
497 signals was set at 10-fold the analytical precision of the instruments (Langdon et al., 2010) for
498 A_T and Ca^{2+} measurements (1.2 and 2.9 µmol kg^{-1}, respectively) and above the detection limit
499 of 15 cpm for ^{45}Ca activity estimated. Maximum incubation times are more difficult to
500 estimate. Langdon et al. (2010) and Riebesell et al. (2010) recommend considering incubation
501 times short enough to maintain A_T and C_T within an acceptable range (ΔA_T and ΔC_T < 10%).
502 As it is more difficult to estimate what changes in pH are acceptable, we have arbitrarily
503 considered a maximal change in pH of 0.06, corresponding to the lowest change in global
504 surface ocean pH projected for 2100 (IPCC, 2014). Maximal incubation times, as presented in
505 Table 5 (t_{max}), correspond then to incubation times that should not be exceeded in order to
506 maintain acceptable conditions of the carbonate chemistry (ΔpH_T < 0.6 and ΔA_T < 10% and
507 ΔC_T < 10%).

508 Under light and ambient pH conditions, even if the ratio between incubation volume
509 and nubbin size is much higher than for previous similar studies (e.g. Cohen et al., 2017), all
510 methods would allow a precise estimation of calcification rates over very short incubation
511 times (~15 min to 1 h, depending on the method) while leading to moderate changes in
512 carbonate chemistry. In the dark, and under ambient pH conditions, in the absence of pH
513 increase due to photosynthesis, the decrease of pH due to respiration, narrows the possible
514 incubation period to 1.3 h. While this is still larger than the incubation time allowing to obtain
515 a significant signal with the alkalinity anomaly technique (~20 min), the other two methods
516 necessitate longer incubation times to obtain precise estimates (> 1.5 h). At lower pH, both
517 under light and dark conditions, and using open systems without a continuous pH regulation
518 as in our study, it is obvious that all techniques are not well adapted to this experimental
519 protocol. Indeed, as a consequence of lower calcification rates at lower pH and significant

520 CO_2 degassing, incubation times necessary to obtain significant signals using these techniques
521 are too large to maintain the carbonate parameters within an acceptable range. This is not
522 insurmountable as a continuous regulation of pH using for instance pure CO_2 bubbling or
523 incubations performed in a closed container (i.e. without contact to the atmosphere) would
524 alleviate these problems.

525 In conclusion, the present study is the first one allowing a direct (i.e. during the same
526 incubations) comparison of three methods used to estimate coral calcification rates, the
527 calcium and alkalinity anomaly techniques and the ^{45}Ca incorporation technique. These
528 methods provided very consistent calcification rates of the coral *Stylophora pistillata*
529 independently of the conditions set for the incubations (light vs. dark, ambient vs. low pH).
530 Among these three methods, the alkalinity anomaly and the ^{45}Ca incorporation techniques
531 appear to be the most sensitive allowing the quantification of coral calcification rates without
532 significant changes in targeted environmental conditions. In contrast, the ^{13}C incorporation
533 technique did not provide reliable calcification rates and its use is not recommended until
534 further investigations clarify the discrepancies. Finally, this study was restricted to a single
535 coral species and used nubbins fully covered with tissues. Conducting similar comparison
536 studies with other coral species as well as other major calcifying groups widely studied in the
537 context of ocean acidification (e.g. coralline algae, molluscs etc…) would be necessary for a
538 better understanding of ocean acidification impacts on ecosystem services provided by
539 calcifying organisms.

Acknowledgements

This work was supported by the IAEA's Ocean Acidification International Coordination Center (OA-ICC) and the IAEA-ICTP Sandwich Training Educational Programme (STEP) and Project "Strengthening the National System for Analysis of the Risks and Vulnerability of Cuban Coastal Zone Through the Application of Nuclear and Isotopic Techniques" National Program PNUOLU /4-1/ 2 No. /2017 of the National Nuclear Agency (AENTA). We thank the Monaco government, the Centre Scientifique de Monaco for propagating and maintaining the coral nubbins and Samir Alliouane for technical assistance for total alkalinity and calcium measurements.

REFERENCES

Albright, R., Caldeira, L., Hosfelt, J., Kwiatkowski, L., Maclaren, J. K., Mason, B. M., Nebuchina, Y., Ninokawa, A., Pongratz, J., Ricke, K. L., Rivlin, T., Schneider, K., Sesboüé, M., Shamberger, K., Silverman, J., Wolfe, K., Zhu, K., and Caldeira, K.: Reversal of ocean acidification enhances net coral reef calcification, Nature, 531, 362, 10.1038/nature17155, 2016.

Albright, R., Takeshita, Y., Koweek, D. A., Ninokawa, A., Wolfe, K., Rivlin, T., Nebuchina, Y., Young, J., and Caldeira, K.: Carbon dioxide addition to coral reef waters suppresses net community calcification, Nature, 555, 516, 10.1038/nature25968, 2018.

Cao, Z., and Dai, M.: Shallow-depth $CaCO_3$ dissolution: Evidence from excess calcium in the South China Sea and its export to the Pacific Ocean, Global Biogeochemical Cycles, 25, doi:10.1029/2009GB003690, 2011.

Chisholm, J. R. M., and Gattuso, J.-P.: Validation of the alkalinity anomaly technique for investigating calcification and photosynthesis in coral reef communities, Limnology and Oceanography, 36, 1232-1239, 1991.

Cohen, S., Krueger, T., and Fine, M.: Measuring coral calcification under ocean acidification: methodological considerations for the ^{45}Ca-uptake and total alkalinity anomaly technique, PeerJ, 5, e3749, 10.7717/peerj.3749, 2017.

Cyronak, T., Andersson, A. J., Langdon, C., Albright, R., Bates, N. R., Caldeira, K., Carlton, R., Corredor, J. E., Dunbar, R. B., Enochs, I., Erez, J., Eyre, B. D., Gattuso, J.-P., Gledhill, D., Kayanne, H., Kline, D. I., Koweek, D. A., Lantz, C., Lazar, B., Manzello, D., McMahon, A., Meléndez, M., Page, H. N., Santos, I. R., Schulz, K. G., Shaw, E., Silverman, J., Suzuki, A., Teneva, L., Watanabe, A., and Yamamoto, S.: Taking the

572 metabolic pulse of the world's coral reefs, PLOS ONE, 13, e0190872,
573 10.1371/journal.pone.0190872, 2018.
574 Dickson, A. G., Sabine, C. L., and Christian, J. R.: Guide to best practices for ocean CO_2
575 measurements. PICES Special Publication 3, 191pp, 2007.
576 Erez, J.: Vital effect on stable-isotope composition seen in foraminifera and coral skeletons,
577 Nature, 273, 199-202, 10.1038/273199a0, 1978.
578 Furla, P., Galgani, I., Durand, I., and Allemand, D.: Sources and mechanisms of inorganic
579 carbon transport for coral calcification and photosynthesis, Journal of Experimental
580 Biology, 203, 3445-3457, 2000.
581 Gattuso, J.-P., and Hansson, L.: Ocean acidification: background and history, in: Ocean
582 acidification, edited by: Gattuso, J.-P., and Hansson, L., Oxford University Press,
583 Oxford, 1-20, 2011.
584 Gazeau, F., Urbini, L., Cox, T. E., Alliouane, S., and Gattuso, J. P.: Comparison of the
585 alkalinity and calcium anomaly techniques to estimate rates of net calcification, Marine
586 Ecology Progress Series, 527, 1-12, 2015.
587 Gillikin, D. P., and Bouillon, S.: Determination of $\delta^{18}O$ of water and $\delta^{13}C$ of dissolved
588 inorganic carbon using a simple modification of an elemental analyser-isotope ratio
589 mass spectrometer: an evaluation, Rapid Communications in Mass Spectrometry, 21,
590 1475-1478, doi:10.1002/rcm.2968, 2007.
591 Goreau, T. F.: The physiology of skeleton formation in corals. I. A method for measuring the
592 rate of calcium deposition by corals under different conditions, Biological Bulletin, 116,
593 59-75, 1959.
594 Goreau, T. F., and Bowen, V. T.: Calcium uptake by a coral, Science, 122, 1188-1189,
595 10.1126/science.122.3181.1188, 1955.

596 Houlbrèque, F., Reynaud, S., Godinot, C., Oberhänsli, F., Rodolfo-Metalpa, R., and Ferrier-
597 Pagès, C.: Ocean acidification reduces feeding rates in the scleractinian coral
598 *Stylophora pistillata*, Limnology and Oceanography, 60, 89-99, doi:10.1002/lno.10003,
599 2015.
600 IPCC: Climate Change 2014: Synthesis Report. Contribution of Working Groups I, II and III
601 to the Fifth Assessment Report of the Intergovernmental Panel on Climate Change,
602 edited by: Team, C. W., Pachauri, R. K., and Meyer, L. A., IPCC, Geneva, Switzerland,
603 151 pp., 2014.
604 Jokiel, P. L., Maragos, J. E., and Franzisket, L.: Coral growth: buoyant weight technique, in:
605 Coral reefs: research methods, edited by: Stoddart, D. R., and Johannes, R. E., Paris:
606 Unesco, 379-396, 1978.
607 Langdon, C., Gattuso, J.-P., and Andersson, A. J.: Measurements of calcification and
608 dissolution of benthic organisms and communities, in: Guide to Best Practices for
609 Ocean Acidification Research and Data Reporting, 213-234, 2010.
610 Le Quéré, C., Andrew, R. M., Friedlingstein, P., Sitch, S., Hauck, J., Pongratz, J., Pickers, P.
611 A., Korsbakken, J. I., Peters, G. P., Canadell, J. G., Arneth, A., Arora, V. K., Barbero,
612 L., Bastos, A., Bopp, L., Chevallier, F., Chini, L. P., Ciais, P., Doney, S. C., Gkritzalis,
613 T., Goll, D. S., Harris, I., Haverd, V., Hoffman, F. M., Hoppema, M., Houghton, R. A.,
614 Hurtt, G., Ilyina, T., Jain, A. K., Johannessen, T., Jones, C. D., Kato, E., Keeling, R. F.,
615 Goldewijk, K. K., Landschützer, P., Lefèvre, N., Lienert, S., Liu, Z., Lombardozzi, D.,
616 Metzl, N., Munro, D. R., Nabel, J. E. M. S., Nakaoka, S. I., Neill, C., Olsen, A., Ono,
617 T., Patra, P., Peregon, A., Peters, W., Peylin, P., Pfeil, B., Pierrot, D., Poulter, B.,
618 Rehder, G., Resplandy, L., Robertson, E., Rocher, M., Rödenbeck, C., Schuster, U.,
619 Schwinger, J., Séférian, R., Skjelvan, I., Steinhoff, T., Sutton, A., Tans, P. P., Tian, H.,

Tilbrook, B., Tubiello, F. N., van der Laan-Luijkx, I. T., van der Werf, G. R., Viovy, N., Walker, A. P., Wiltshire, A. J., Wright, R., Zaehle, S., and Zheng, B.: Global Carbon Budget 2018, Earth Syst. Sci. Data, 10, 2141-2194, 10.5194/essd-10-2141-2018, 2018.

Lebel, J., and Poisson, A.: Potentiometric determination of calcium and magnesium in seawater, Marine Chemistry, 4, 321–332, doi:10.1016/0304- 4203(76)90018-9, 1976.

Marshall, A. T., and Wright, A.: Coral calcification: autoradiography of a scleractinian coral *Galaxea fascicularis* after incubation in ^{45}Ca and ^{14}C, Coral Reefs, 17, 37-47, 10.1007/s003380050092, 1998.

McCoy, S. J., Pfister, C. A., Olack, G., and Colman, A. S.: Diurnal and tidal patterns of carbon uptake and calcification in geniculate inter-tidal coralline algae, Marine Ecology, 37, 553-564, doi:10.1111/maec.12295, 2016.

Murillo, L. J. A., Jokiel, P. L., and Atkinson, M. J.: Alkalinity to calcium flux ratios for corals and coral reef communities: variances between isolated and community conditions, PeerJ, 2, e249, 10.7717/peerj.249, 2014.

Orr, J. C., Epitalon, J.-M., Dickson, A. G., and Gattuso, J.-P.: Routine uncertainty propagation for the marine carbon dioxide system, Marine Chemistry, 207, 84-107, https://doi.org/10.1016/j.marchem.2018.10.006, 2018.

Riebesell, U., Fabry, V. J., Hansson, L. and Gattuso, J.-P.: Guide to best practices for ocean acidification research and data reporting, Rep. Int. Res. Work. best Pract. Ocean Acidif. Res. (19-21 Novemb. 2008 Kiel, Ger., (July), 260 p, doi:10.2777/58454, 2010.

Schoepf, V., Hu, X., Holcomb, M., Cai, W.-J., Li, Q., Wang, Y., Xu, H., Warner, M. E., Melman, T. F., Hoadley, K. D., Pettay, D. T., Matsui, Y., Baumann, J. H., and Grottoli, A. G.: Coral calcification under environmental change: a direct comparison of the

alkalinity anomaly and buoyant weight techniques, Coral Reefs, 36, 13-25, 10.1007/s00338-016-1507-z, 2017.

Smith, S. V., and Key, G. S.: Carbon dioxide and metabolism in marine environments, Limnology and Oceanography, 20, 493-495, 1975.

Smith, S. V., and Kinsey, D. W.: Calcification and organic carbon metabolism as indicated by carbon dioxide, in: Coral reefs: Research methods, edited by: Stoddart, D. R., and Johannes, R. E., Monogr. Oceanogr. Methodol. 5. UNESCO, 1978.

Sokal, R. R., and Rohlf, F. J.: Biometry, the principles and practice of statistics in biological research, 3rd ed. W. H. Freeman, New York, 1995.

Tambutté, E., Allemand, D., Bourge, I., Gattuso, J.-P., and Jaubert, J.: An improved Ca^{45} protocol for investigating physiological mechanisms in coral calcification, Marine Biology, 122, 453-459, 10.1007/bf00350879, 1995.

Wolf-Gladrow, D. A., Zeebe, R. E., Klaas, C., Körtzinger, A., and Dickson, A. G.: Total alkalinity: the explicit conservative expression and its application to biogeochemical processes, Marine Chemistry, 106, 287-300, doi:10.1016/j.marchem.2007.01.006, 2007.

659 Table 1. Experimental details for the series of incubations of the coral *Stylophora pistillata* performed under ambient and low pH, and in
660 the light and dark following ^{45}Ca or ^{13}C labelling. The ratio W_w:W_c corresponds to the ratio between seawater weight (g) and skeletal dry
661 weight (g). Values represent mean ± standard deviation (SD); n is the number of true replicates considered for each experiment. All
662 incubations were conducted at 25 ± 0.5 °C.

pH conditions	Ambient (n = 6)				Lowered (n = 5)	
Added label	^{45}Ca		^{13}C		^{45}Ca	
Light conditions	Light	Dark	Light	Dark	Light	Dark
Coral size (mm)	33.2 ± 1.5	44.7 ± 1.5	36.3 ± 2.2	50.2 ± 1.7	26.0 ± 1.6	28.9 ± 1.9
Coral Skeleton dry weight (g)	2.5 ± 0.5	3.8 ± 0.7	2.6 ± 0.5	4.7 ± 0.5	2.1 ± 0.2	2.8 ± 0.4
Ratio W_w:W_c	126.4 ± 25.6	81.9 ± 14.7	106.9 ± 24.5	67.8 ± 7.5	146.5 ± 14.3	110.0 ± 12.4
Incubation time (h)	8	8	9.12	9.12	5	11

663

Table 2. Environmental conditions at the start of incubations of the coral *Stylophora pistillata*. pH on the total scale (pH_T), partial pressure of CO_2 (pCO_2 in µatm), total alkalinity (A_T in µmol kg^{-1}), dissolved inorganic carbon (C_T in µmol kg^{-1}), saturation states with respect to aragonite (Ω_a) and calcite (Ω_c) as well as calcium concentrations ($[Ca^{2+}]$ in µmol kg^{-1}) are presented. Labelled seawater ^{45}Ca activity ($Activity_{seawater}$ in Bq mL^{-1}) and the isotopic level, after enrichment, of the seawater dissolved inorganic carbon pool ($\delta^{13}C$-C_T in ‰) are also shown. Means ± standard deviation (SD) of analytical triplicates (duplicates for $\delta^{13}C$-C_T) are shown when available. All incubations were conducted at 25 ± 0.5 °C.

pH conditions	Ambient				Lowered	
Added label	^{45}Ca		^{13}C		^{45}Ca	
Light conditions	Light	Dark	Light	Dark	Light	Dark
pH_T	8.05	8.05	8.06	8.05	7.21	7.24
pCO_2	427.6 ± 8.2	438.8 ± 8.5	425.6 ± 8.2	424.1 ± 8.2	3,727.2 ± 66.8	3,460.1 ± 62.1
A_T	2,556.0 ± 0.5	2,620.0 ± 0.7	2,615.2 ± 0.6	2,535.9 ± 1.8	2,558.4 ± 0.3	2,552.9 ± 2.4
C_T	2,206.4 ± 7.4	2,264.1 ± 7.6	2,252.9 ± 7.7	2,188.2 ± 7.6	2,597.1 ± 2.5	2,579.8 ± 3.5
Ω_a	3.9 ± 0.2	4.0 ± 0.2	4.1 ± 0.2	3.9 ± 0.2	0.7 ± 0.0	0.8 ± 0.0
Ω_c	5.9 ± 0.3	6.1 ± 0.3	6.2 ± 0.3	5.9 ± 0.3	1.1 ± 0.1	1.2 ± 0.1
$[Ca^{2+}]$	11,179.6 ± 0.0	11,164.0 ± 2.0	11,096.5 ± 13.4	11,098.5 ± 2.8	11,281.2 ± 5.5	11,277.6 ± 0.3
$Activity_{seawater}$	16.6	15.1	-	-	28.5	30.4
$\delta^{13}C$-C_T	-	-	1,740 ± 4.7	1,634 ± 11	-	-

Table 3. Changes in total alkalinity (A_T) and calcium concentrations ($[Ca^{2+}]$) during the different types of incubations as compared to control beakers: $\Delta A_T = A_{T2} - A_{T2c}$, $\Delta[Ca^{2+}] = Ca_2 - Ca_{2c}$, both expressed in µmol kg^{-1}. Standard errors (SE) have been calculated as $\sqrt{SE_{AT_2}^2 + SE_{AT_{2c}}^2}$ and $\sqrt{SE_{Ca_2}^2 + SE_{Ca_{2c}}^2}$ for A_T and $[Ca^{2+}]$, respectively, where SE correspond to standard errors associated with the measurement of three analytical replicates per sample. ^{45}Ca activity ($Activity_{sample}$ in Bq) and ^{13}C incorporation ($\delta^{13}C_M$ in ‰) of sampled corals are also shown. Values of ^{45}Ca activity and $\delta^{13}C$ are mean ± standard error of the mean (SE) associated with the measurement of three aliquots for each coral. Outliers (n = 4; see text for details) are identified with an asterisk.

Experiment	Beaker#	ΔA_T	SE ΔA_T	$\Delta[Ca^{2+}]$	SE $\Delta[Ca^{2+}]$	$Activity_{sample}$	$SEActivity_{sample}$	$\delta^{13}C_M$	SE $\delta^{13}C_M$
Ambient pH - ^{45}Ca - Light	1	-343.6	1.3	-166.0	6.0	78.5	1.9	-	-
	2	-368.9	0.9	-174.1	5.1	86.5	2.9	-	-
	3	-336.9	0.9	-181.3	2.7	78.2	2.3	-	-
	4	-364.3	0.9	-190.6	6.3	85.2	0.8	-	-
	5	-406.7	0.7	-225.6	1.4	95.7	2.6	-	-
	6	-407.5	1.2	-175.9	1.1	100.6	3.5	-	-
Ambient pH - ^{13}C - Light	1	-386.3	1.5	-195.0	3.8	-	-	-1.4	2.0
	2	-422.6	1.3	-206.8	4.2	-	-	1.8	3.2

	3	-405.4	1.9	-200.9	2.1	-	-	3.4	5.1
	4	-481.6	1.3	-253.2	2.0	-	-	1.1	2.0
	5	-498.4	1.3	-260.5	5.7	-	-	0.8	0.7
	6	-618.1	1.8	-317.7	4.4	-	-	0.1	1.8
Ambient pH - ^{13}C - Dark	1	-300.5	1.4	-168.9	0.6	-	-	-0.3	1.3
	2	-440.8	1.4	-220.7	2.5	-	-	-3.0	0.5
	3	-223.5	1.9	-135.1	0.8	-	-	-3.1	0.6
	4	-347.3	1.1	-185.3	0.2	-	-	0.5	5.4
	5	-571.7	1.3	-301.7	1.2	-	-	0.6	2.1
	6	-434.5	1.3	-224.6	3.7	-	-	0.7	6.1
Ambient pH - ^{45}Ca - Dark	1	-290.2	1.6	-157.9	2.2	56.44	1.24	-	-
	2	-274.3	1.2	-130.4	4.4	50.1	0.74	-	-
	3	-300.8	1.3	-168.3	0.9	57.17	1.75	-	-
	4	-327.0	2.7	-139.3	5.3	66.24	0.69	-	-
	5	-342.8	1.2	-172.6	3.0	68.37	3.11	-	-
	6	-228.3	1.8	-113.4	2.5	52.36	2.49	-	-

Lowered pH - ^{45}Ca - Light	1	-59.3	2.2	-1.6*	6.9	20.2	0.7	-	-
	2	-44.2	2.2	-11.0	2.2	15.3	0.4	-	-
	3	-71.3	2.8	-28.0	5.9	22.5	0.3	-	-
	4	-70.2	2.4	-35.7	7.6	23.4	0.4	-	-
	5	-56.4	2.5	-19.6	7.1	20	0.9	-	-
Lowered pH - ^{45}Ca - Dark	1	-745.6*	13.2	0.8*	0.3	14.5	0.2	-	-
	2	-52.4	2.1	-1.0*	1.0	22.1	0.3	-	-
	3	-50.5	2.1	-22.5	2.8	22.1	0.1	-	-
	4	-54.3	2.1	-30.3	8.5	23.3	0.4	-	-
	5	-99.4	2.1	-32.8	4.1	16.1	0.1	-	-

677

678 Table 4. Model-II regression results of the comparison between calcification rates estimated using the different methods considered in this
679 study: the alkalinity and calcium anomaly techniques (G_{AT} and G_{Ca}, respectively) as well as the ^{45}Ca and ^{13}C incorporation techniques
680 (G_{45Ca} and G_{13C}, respectively). The number of samples (n), the regression coefficient (R^2), the slope and intercept (including their 95%
681 confidence intervals, 95% CI), as well as p value are shown for each comparison. Few identified outliers (n = 4) have been removed from
682 the analyses, see Table 3 and Table A1.

Methods compared	n	R^2	Slope			Intercept			p value
			Value	95% CI		Value	95% CI		
				Low	High		Low	High	
G_{AT} vs. G_{Ca}	32	0.98	0.95	0.90	1.00	0.09	0.00	0.18	$4.9\ e^{-27}$
G_{AT} vs. G_{45Ca}	21	0.99	0.94	0.90	0.98	0.09	0.03	0.15	$3.9\ e^{-21}$
G_{Ca} vs. G_{45Ca}	20	0.97	1.00	0.91	1.09	-0.06	-0.20	0.07	$5.9e-^{15}$
G_{AT} vs. G_{13C}	12	0.33	0.49	0.05	1.2	0.77	-1.2	2.1	0.0506
G_{Ca} vs. G_{13C}	12	0.32	0.46	0.03	1.1	0.94	-0.9	2.2	0.0551

683

Table 5. Incubation times (t_{min}; h) necessary to obtain significant signals using the three methods: the alkalinity anomaly technique (A_T), the calcium anomaly technique (Ca^{2+}) and the ^{45}Ca incorporation techniques (^{45}Ca), see text for calculation procedures. t_{max} (h) is the maximum incubation time to maintain carbonate chemistry within an acceptable range ($\Delta pH_T < 0.06$ and $\Delta C_T < 10\%$ and $\Delta A_T < 10\%$). The ratios between incubation volume (in mL) and the size of the nubbins (in cm), considered in our study for the different sets of incubations (Ambient pH vs. Low pH; Light vs. Dark), are also shown. t_{min} values are noted in bold when higher than t_{max}.

	Ratio V:S	t_{min} (h)			t_{max} (h)
		A_T	Ca^{2+}	^{45}Ca	
Ambient pH – Light	77-95	0.26	1.00	0.6	4.7
Ambient pH – Dark	59-69	0.33	**2.10**	**1.5**	1.3
Lowered pH – Light	109-121	**1.25**	**6.15**	**1.1**	0.5
Lowered pH – Dark	95-109	**1.60**	**11.20**	**3.4**	1.3

690 # Figure captions

691 Fig. 1. Scheme of the polyethylene container in which a coral nubbin is suspended with a
692 nylon line and covered with a transparent film.

693 Fig. 2. Calcification rates estimated based on the alkalinity anomaly technique (G_{AT}) as a
694 function of calcification rates estimated based on the calcium anomaly technique (G_{Ca}). The
695 dashed line represents the 1:1 relationship while the full line represents the model-II
696 regression relationship. Horizontal error bars represent standard errors (SE) associated with
697 the estimation of G_{Ca}. Vertical error bars representing SE associated with the estimation of
698 G_{AT} are too small to be visible. The corresponding dataset can be found in Table A1.

699 Fig. 3. Calcification rates estimated based on the alkalinity anomaly technique (G_{AT}) as a
700 function of calcification rates estimated based on the ^{45}Ca incorporation technique (G_{45Ca}).
701 The dashed line represents the 1:1 relationship while the full line represents the model-II
702 regression relationship. Horizontal error bars represent standard errors (SE) associated with
703 the estimation of G_{45Ca}. Vertical error bars representing SE associated with the estimation of
704 G_{AT} are too small to be visible. The corresponding dataset can be found in Table A1.

705 Fig. 4. Calcification rates estimated based on the alkalinity anomaly technique (G_{AT}) as a
706 function of calcification rates estimated based on ^{13}C incorporation technique (G_{13C}). The
707 dashed line represents the 1:1 relationship while the full line represents the model-II
708 regression relationship. Horizontal error bars represent standard errors (SE) associated with
709 the estimation of G_{13C}. Vertical error bars representing SE associated with the estimation of
710 G_{AT} are too small to be visible. The corresponding dataset can be found in Table A1.

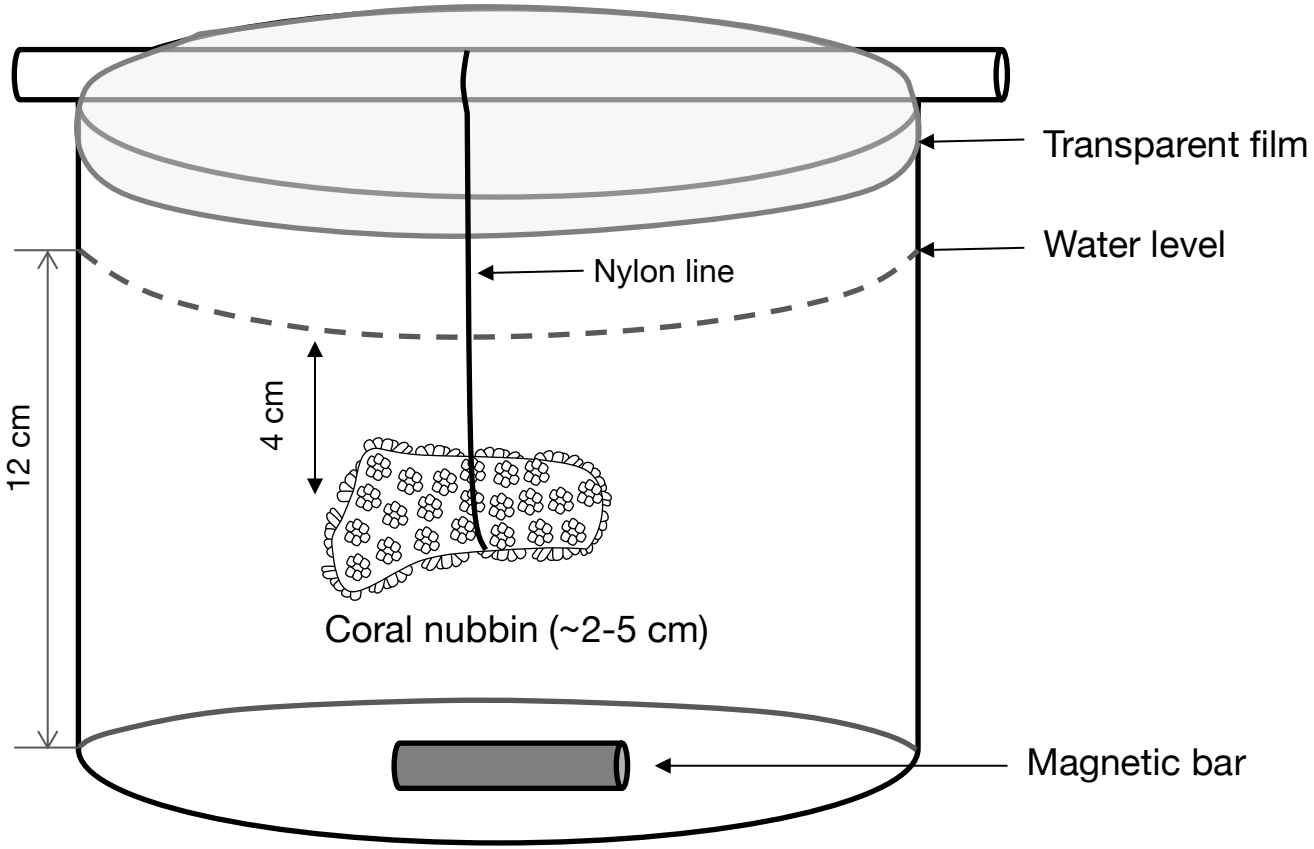
Transparent film
Water level
Nylon line
12 cm
4 cm
Coral nubbin (~2-5 cm)
Magnetic bar

711

712 Fig. 1.

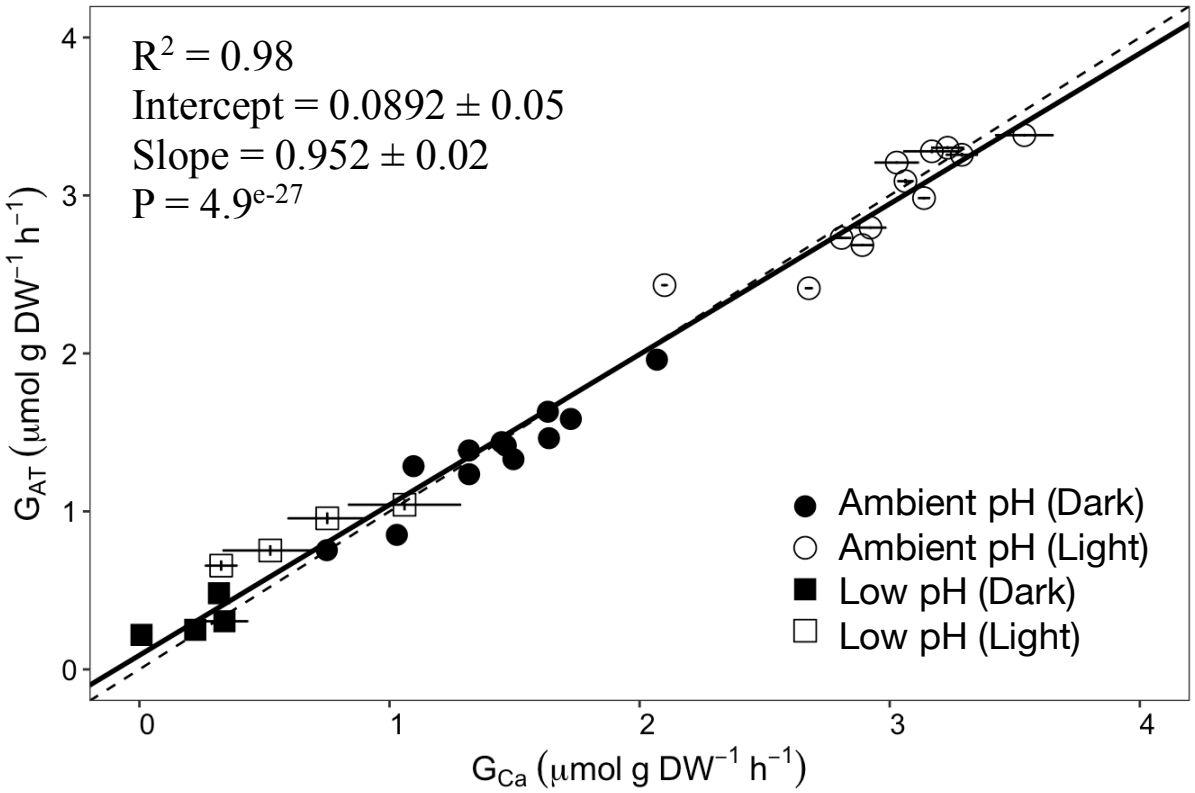
R2 = 0.98
Intercept = 0.0892 ± 0.05
Slope = 0.952 ± 0.02
P = 4.9e-27
Ambient pH (Dark)
Ambient pH (Light)
Low pH (Dark)
Low pH (Light)
GAT (μmol g DW−1 h−1)
GCa (μmol g DW−1 h−1)
0
1
2
3
4

713

714 Fig. 2.

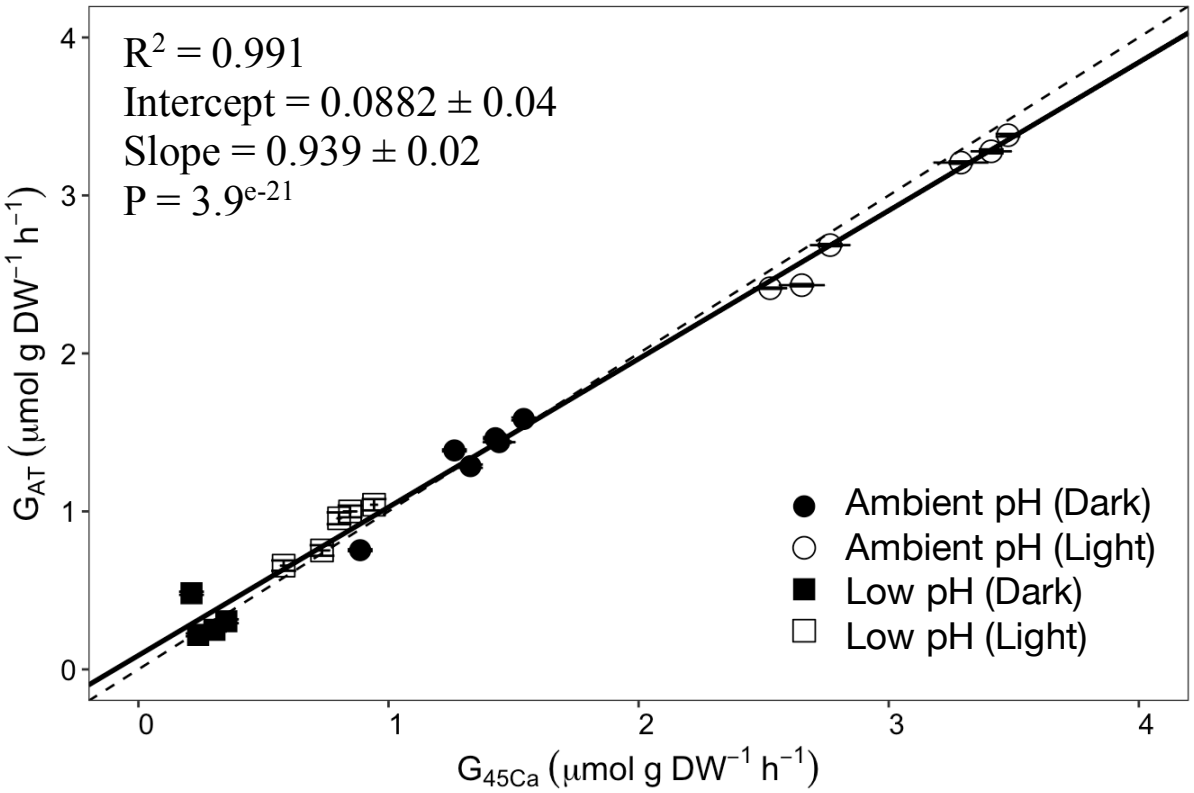
R2 = 0.991
Intercept = 0.0882 ± 0.04
Slope = 0.939 ± 0.02
P = 3.9e-21
Ambient pH (Dark)
Ambient pH (Light)
Low pH (Dark)
Low pH (Light)
GAT (μmol g DW−1 h−1)
G45Ca (μmol g DW−1 h−1)
0
1
2
3
4

715

716 Fig. 3.

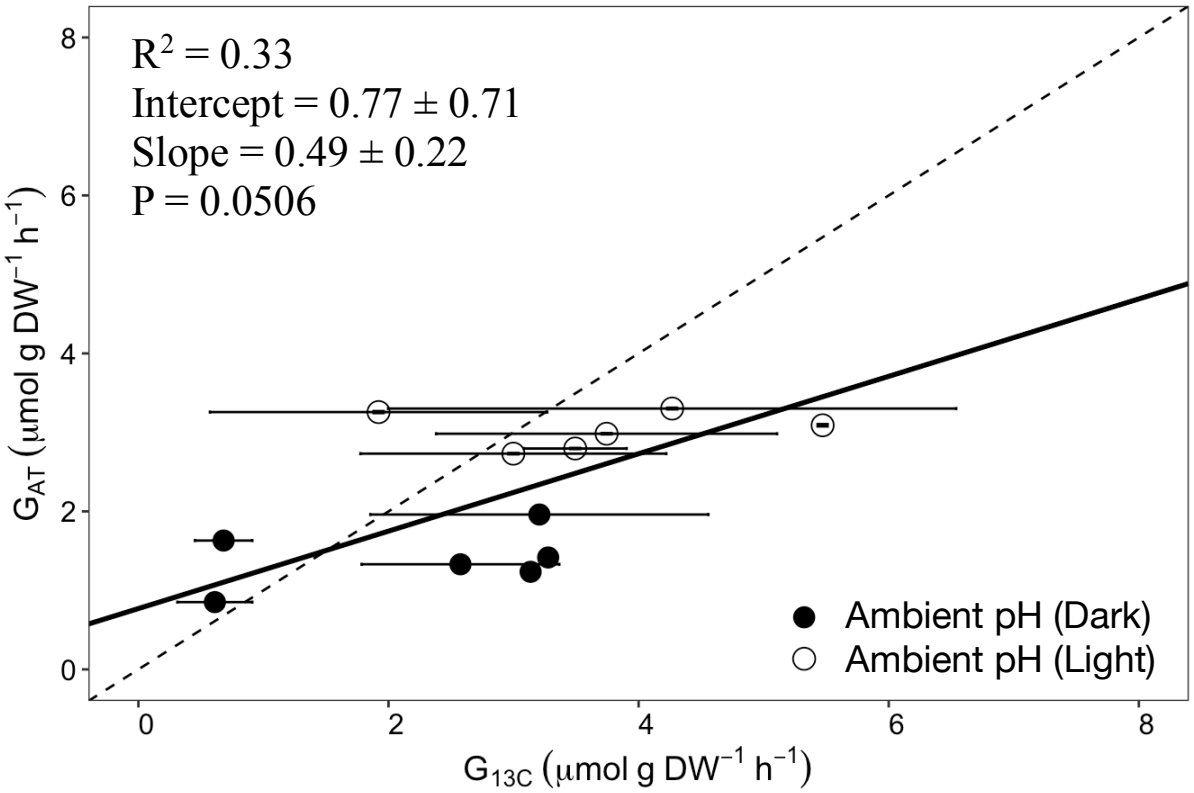
R2 = 0.33
Intercept = 0.77 ± 0.71
Slope = 0.49 ± 0.22
P = 0.0506
Ambient pH (Dark)
Ambient pH (Light)
GAT (μmol g DW−1 h−1)
G13C (μmol g DW−1 h−1)
0
2
4
6
8

717

718 Fig. 4.